Journal of Experimental Nanoscience

ISSN: 1745-8080 (Print) 1745-8099 (Online) Journal homepage: https://www.tandfonline.com/loi/tjen20

Fabrication of PtNi bimetallic nanoparticles supported on multi-walled carbon nanotubes

Walid M. Daoush & Toyoko Imae

To cite this article: Walid M. Daoush & Toyoko Imae (2015) Fabrication of PtNi bimetallic nanoparticles supported on multi-walled carbon nanotubes, Journal of Experimental Nanoscience, 10:5, 392-406, DOI: 10.1080/17458080.2013.838703

To link to this article: https://doi.org/10.1080/17458080.2013.838703

Journal of Experimental Nanoscience, 2015
Vol. 10, No. 5, 392–406, http://dx.doi.org/10.1080/17458080.2013.838703

Taylor & Francis
Taylor & Francis Group

Fabrication of PtNi bimetallic nanoparticles supported on multi-walled carbon nanotubes

Walid M. Daoush[a]* and Toyoko Imae[b]

[a]*Department of Production Technology at the Faculty of Industrial Education, Helwan University, Cairo, Egypt;* [b]*Graduate Institute of Applied Science and Technology, Honors College, National Taiwan University of Science and Technology, Taipei 10607, Taiwan (ROC)*

(*Received 11 July 2013; final version received 24 August 2013*)

Platinum/nickel bimetallic nanoparticles supported on multi-walled carbon nanotubes (*x*PtNi/CNTs) were synthesised. The fabrication process includes the chemical modification on the graphene surface of CNTs by acid treatment and the subsequent deposition of Pt or PtNi bimetallic nanoparticles with different compositions of Pt (x = 100, 90, 80 and 70 wt%). The deposition was carried out using ethylene glycol as a reducing agent in the polyol method or using poly (amidoamine) dendrimer as a platform and sodium borohydride as a reducing agent to load the metal nanoparticles on the CNT surface. The structures of the produced PtNi/CNT nanoparticles were investigated by ultraviolet absorption spectra, X-ray diffraction (XRD) and the composite ratio consisting of 70 wt% of metal content and 30 wt% of CNTs was confirmed by the thermogravimetric analysis. The morphology and the phase identification of the produced PtNi/CNT nanoparticles were investigated by high-resolution scanning electron microscope, transmission electron microscope and XRD measurements. It was observed that the deposited Pt and PtNi bimetallic nanoparticles on the surface of CNTs had average particle sizes of 2–16 nm, when they were prepared from the polyol method. On the other hand, the PtNi/CNT nanoparticles prepared by using a dendrimer as an intermediate had a smaller particle size and more uniform size distribution of the quantum dot size ranged from 2 to 4 nm.

Keywords: carbon nanotube; bimetallic nanoparticle; polyol method; dendrimer

1. Introduction

Fuel cells have attracted attention as an important power source for the future because of their high energy conversion efficiency and low environmental pollution. On the conversion of chemical energy into electricity in direct methanol fuel cells, the development of better catalysts to improve the cell performance is required. Noble metals, such as Pt, supported on carbons with wide surface area, are typically used as electrocatalysts for several kinds of fuel cells.[1–3] To date, the performance of current fuel cells is still limited due to high overpotential and slow kinetics for oxygen reduction reaction at cathode.[4] Meanwhile the resultant high cost is also one of the obstacles preventing the popular usage of fuel cells. In order to reduce the cost, one method is to prepare Pt nanoparticles supported on carbon, which helps to lower the platinum loading in the fuel cells.[5,6]

*Corresponding author. Email: waliddaoush@techedu.helwan.edu.eg

Another approach is to synthesise platinum-based binary or ternary electrocatalysts. As example, Ru,[7,8] Mo [9] and Cu [10] have been used as catalysts together with Pt. There is an increasing attention in PtNi alloys because of their lower material cost and effective resistance to dissolution in electrolytes. It has been reported that PtNi alloys are promising catalysts for the oxygen reduction reaction.[11–16]

Currently, the durability of Pt alloy catalysts is not satisfactory, because added metal species dissolve under cathodic condition.[17–21] Thus novel methods to improve the durability of carbon-supported Pt metal electrocatalysts are required. In fact, the durability of Pt electrocatalysts is improved to some extent by the addition of another metal. However, it is difficult to obtain alloy catalysts of small particle size, since these catalysts must be treated at high temperatures for alloy formation.

There has been an increasing interest in multi-walled carbon nanotubes (MWCNTs) as heterogeneous catalyst supports,[22–30] owing to their high porosity and high electrical conductivity. However, the role of deposition of bimetallic catalysts on CNTs in supporting the improvement of electrochemical activity in methanol oxidation has not yet been clearly elucidated. Previous study has shown an efficient way to deposit electrocatalysts on the sidewalls of CNTs.[31] Proper dispersion of the catalysts on CNTs would enhance the reaction kinetics and activity for methanol oxidation by the adsorption of the substance (methanol) on the graphene structure in the longitudinal dimension which accelerates the kinetic reaction.

In this paper, a series of (xPtNi/CNTs) (x = 100, 90, 80 and 70 wt%) bimetallic nanoparticles were deposited on the surface of CNTs in order to find out the relationship among the synthesis process, the particle morphology, the particle size and its distribution. CNTs were modified by oxidation reagents to introduce different surface chemical groups on the graphene structure.[32] The PtNi/CNTs bimetallic nanoparticles were primarily prepared by a polyol method using ethylene glycol as a reducing agent for the metal precursors.[33] Second, the PtNi/CNTs bimetallic nanoparticles were prepared by reducing the metal precursors loaded on dendrimers anchored on CNTs with sodium borohydride.[32] Various analyses like Fourier transform infrared (FTIR), ultraviolet–visible (UV–visible) absorption spectrometry, scanning electron microscopy (SEM), transmission electron microscopy (TEM), X-ray diffraction (XRD) and thermogravimetric analysis (TGA) were carried out to characterise the morphology and the properties of the prepared PtNi/CNT nanoparticles. Our results show great promise for a solution of high demand for PtNi/CNT bimetallic nanoparticles in the electrocatalysts of current direct methanol fuel cells.

2. Experimental

2.1. Reagents

Sodium hexachloroplatinate (IV) hexahydrate, nickel (II) chloride and fourth-generation (G4) poly(amidoamine) (PAMAM) dendrimer, 1-ethyl-3-(3-dimethylaminopropyl) carbodiimide (EDAC) were purchased from Aldrich Co. Ltd. Deionised distilled water was used throughout experiments. The CNTs were purchased from Iljin Nanotech Ltd. and purified according to the previous procedure [32]: CNTs (50 mg) were dispersed by sonication and heated at 60 °C in concentrated HCl (50 ml) for 24 h. After settling for 1 h, the CNTs were washed with water by centrifugation followed by decantation for several times and dried at 150 °C for 2 h. Acid-treated CNTs were obtained by dispersing the purified CNTs by

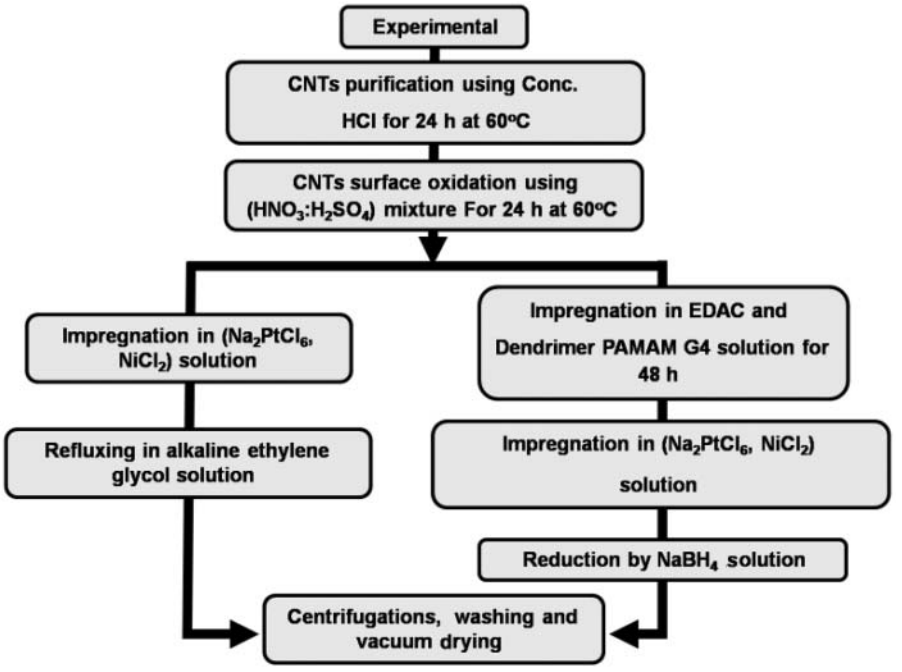

Figure 1. A schematic diagram of the two different syntheses methods of PtNi/CNT nanoparticles.

sonication and heating them in concentrated HNO_3/H_2SO_4 (3:1, v/v) (50 ml) at 60 °C for 24 h. After keeping aside for 24 h for settling acid-treated CNTs, the produced suspension was centrifuged and the supernatant solution was decanted. The product was washed several times with water followed by drying at 150 °C for 2 h. The complete fabrication processes of the Pt/CNT and PtNi/CNT bimetallic nanoparticles are illustrated in Figure 1.

2.2. Synthesis of Pt/CNT and PtNi/CNT bimetallic nanoparticles

The Pt/CNT and the related PtNi/CNT bimetallic materials were fabricated by two different synthesis methods. The total metal-to-carbon ratio was 70:30 by weight per cent. Figure 2 illustrates a schematic diagram of the two synthesis methods of PtNi/CNT nanoparticles.

2.2.1. Synthesis of Pt/CNT and PtNi/CNT nanoparticles by a polyol method

A modified polyol method was used to prepare Pt/CNTs, 90PtNi/CNTs, 80PtNi/CNTs and 70PtNi/CNTs for 100, 90, 80 and 70 wt%, respectively, of Pt in PtNi. A quantity of 1 mg of acid-treated CNTs was added to 2 ml of ethylene glycol solution of sodium hexachloroplatinate (IV) hexahydrate and nickel (II) chloride as precursors of Pt and Ni metals, respectively. The pH was adjusted at 12 using sodium hydroxide. The mixture underwent refluxing overnight. The resultant Pt/CNT and Pt/Ni/CNT nanoparticles were washed with ethyl alcohol, followed by purification (centrifugation/decantation) for several times and drying at 150 °C for 2 h.

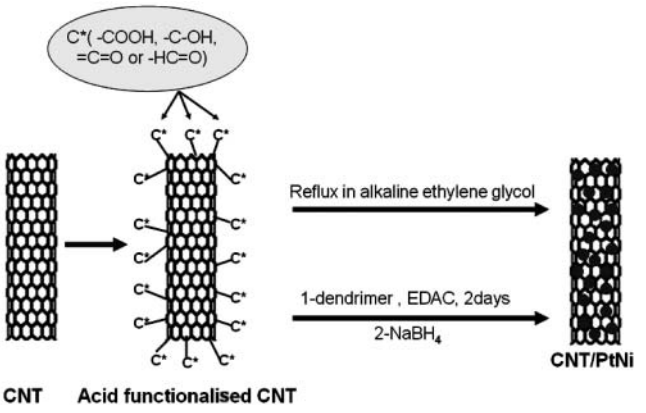

Figure 2. A schematic diagram of two different routes for fabrication of PtNi/CNT nanoparticles.

2.2.2. Synthesis of Pt/CNT and PtNi/CNT nanoparticles using a G4 PAMAM dendrimer

A quantity of 0.5 mg of acid-treated CNTs was added to 5 ml of a dilute solution (1 vol% of a 10 wt% dendrimer solution: 5 vol% of water) of G4 PAMAM dendrimer, followed by reflux for 1 h. A quantity of 0.5 mg of EDAC was added to the mixture and stirred for 48 h by a magnetic stirrer, followed by drop-wise addition of the metal solution of metal precursors (sodium hexachloroplatinate (IV) hexahydrate and nickel (II) chloride) and by stirring for 1 h. Then 20 ml of an aqueous solution containing 1 mg of $NaBH_4$ was added to the mixture drop by drop. The precipitated powders were collected by centrifugation/decantation, washed and dried at 150 °C for 2 h.

2.3. Characterisations of Pt/CNT and PtNi/CNT bimetallic nanoparticles

The acid-treated MWCNTs were investigated by an FTIR analyser of the Nicolet 6700 model as well as by high-resolution scanning electron microscope (HRSEM). The metal/CNT nanoparticles as well as the acid-treated CNTs were investigated by a thermogravimetric analyser of the TGA Q500 model under temperature up to 850 °C at a scan rate of 10 °C/min. A Jasco V-670 series UV spectrometer was used to characterise the UV–visible absorption bands for the prepared metal/CNT nanoparticles. The morphologies and the particle size distributions of the produced nanomaterials were detected by a TEM of the HITACHI H-7000 model. The investigated MWCNTs as well as the prepared PtNi/CNT bimetallic nanoparticles were investigated by XRD with Cu-K_α target with secondary monochromator using diffractometer of the X'Pert Pro PAnalytical (45 KV, 40 mA) model.

3. Results and discussion

The different amounts of as-received MWCNTs were treated in an ultrasonic bath of acidic media for opening the bundles, de-capping and functionalising the graphene surface of MWCNTs. Figure 3(a) and 3(b) shows SEM images with different magnifications for the as-received MWCNTs and the acid-treated MWCNTs, respectively. This process enhances the shortening of the CNT in length as well as the functionalisation of CNTs that raises the preferable dispersion of CNTs in the solution. While the as-received CNTs have the texture

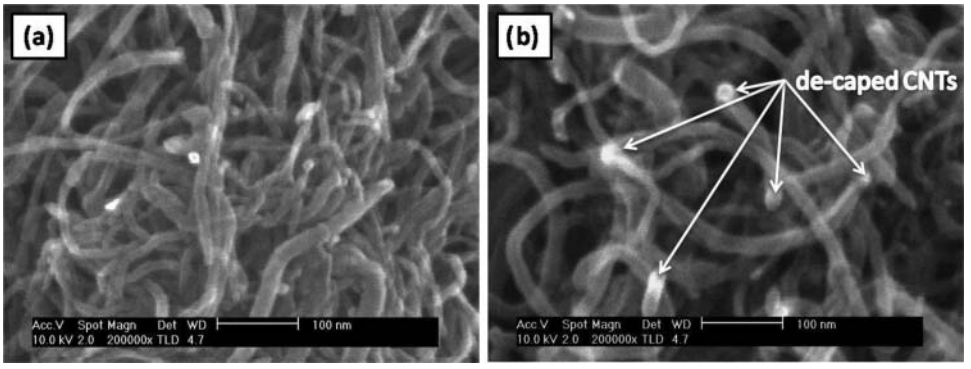

Figure 3. SEM images of the investigated MWNTs: (a) untreated and (b) surface-oxidised MWCNTs.

of agglomerated filaments, after the acid treatment, these agglomerated filaments were partly destroyed and the CNTs were shortened to small segments by the breakage of the chains. As was observed from the literatures for the functionalisation of the carbon allotropies like fullerenes, CNTs and carbon fibers. Introducing hydroxy groups on the graphene structure of CNTs appears to be key to enhance the formation of a uniform coating layer on its surface. Irrespective of the type of the graphene structure, heating a suspension of the fullerenes, carbon fibers and CNTs in nitric acid till it dries gives good results in terms of the growth of nanoparticles around the graphene surface and there is a correlation between the percentage of hydroxyls present on the graphene surface and on the type of growth that occurs on the graphene structure.[34] It has also been reported that the acid-treated CNTs have a shorter length (of approximately 1 μm) than the untreated one due to the stronger reaction of oxidised acids (the acidic mixture of nitric and sulphuric acids) on the graphene structure than nitric acid itself, which introduce several kinds of high oxidation state functional groups and enhance the de-capping and cutting of the CNTs to short segments by introducing carboxylic groups on the graphene structure.[35]

The acid treatments of the MWCNTs by oxidised acids (acidic mixture of nitric and sulphuric acids) modify the surface of the graphene structure by introducing functional groups, such as carboxylic, carbonyl and hydroxyl groups on the CNT surfaces. Figure 4(a)–(d) shows TEM images with different magnifications for the as-received MWCNTs and the acid-treated MWCNTs, respectively. It was observed that the outer walls of the functionalised MWCNTs (Figure 4(d)) have a modified surface due to the surface oxidation by acid treatment process with nitric and sulphuric acid (HNO_3/H_2SO_4) mixture which leads to the breakdown of the C–C bond in the graphene backbones.

The functional groups of the acid-functionalised CNTs were detected by FTIR, as shown in Figure 5. The IR chart indicates seven types of bonding. The first one is the carboxylic group which is detected by the band at wave number of 1710 cm^{-1} due to the C=O double bond and a broadband (at 3443 cm^{-1}) due to the intermolecular hydrogen bonding of O–H in alcohols and carboxylic acids. The second and the third are the C–O groups of alcohols and phenols at 1200 and 1065 cm^{-1}, respectively. In addition, there is a broadband (at 3443 cm^{-1}) of the intermolecular hydrogen bond of the O–H groups. The fourth functional group is the C=C double bond, which was detected by the intensive

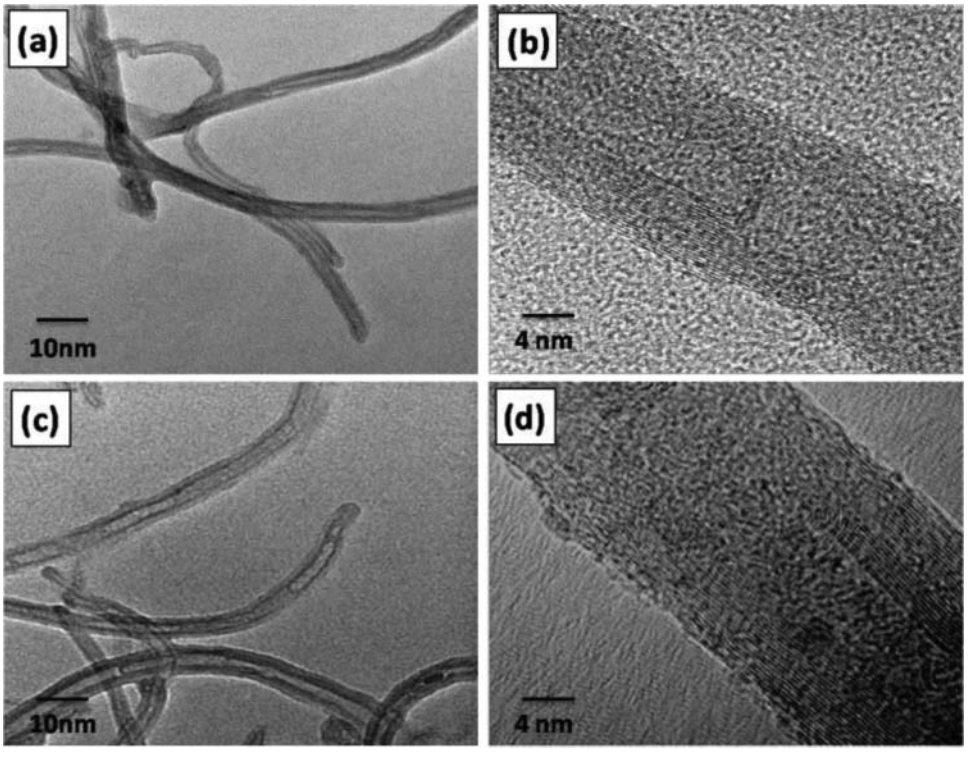

Figure 4. TEM images with different magnifications of untreated (a, b) and acid-treated (c, d) MWCNTs.

band, which appeared at 1638 cm^{-1}, indicating the graphene structure of the CNTs. However, the fifth type of bonding is the C–H bonding for the CHO aldehyde group by the two bands at wave numbers 2950 and 2850 cm^{-1}. Also the sixth type of band is due to the phenyl ring at 600 and 868 cm^{-1}. However, the band of the seventh type of functional group

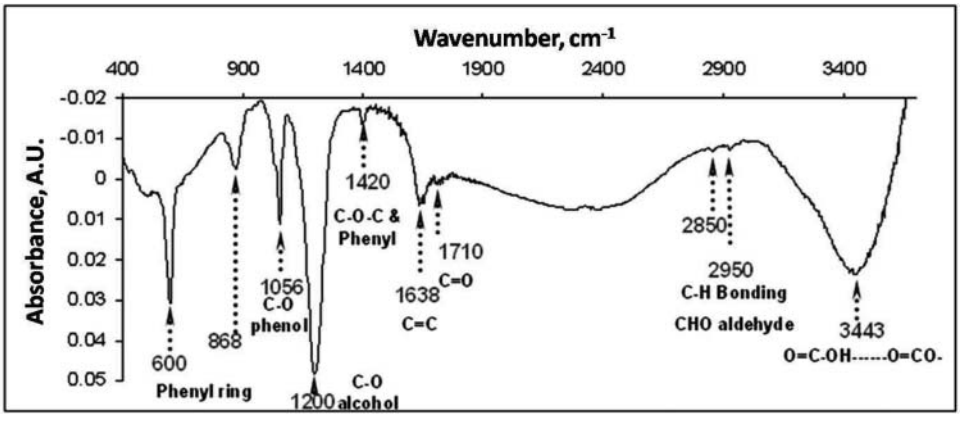

Figure 5. FTIR chart for the acid-functionalised MWCNTs.

is due to the C–O–C bond at 1420 cm^{-1}.[35–40] It was mentioned in the literature that the main surface oxidation of the graphene structure occurred at the de-capped ends of the CNT segments introducing carboxylic groups. However, the aldehydic, ketonic and phenolic groups were introduced at the sidewall of the CNTs due to the oxidation of the conjugated double bonds and the aromatic rings in the graphene chain. This is a characteristic feature for MWCNTs and constitutes backbones for CNTs. In addition, the exchange of a hydrogen atom of the hydrocarbon chain of CNTs by a hydroxyl group is reflected in the FTIR spectrum as absorptions owing to O–H and C–O stretching vibrations.[41]

The acid-treated CNTs underwent Pt and PtNi deposition on their surface by two different methods as illustrated in Figure 2. In the first method, ethylene glycol was used as a reducing agent of platinum and nickel ions in an alkaline sodium hydroxide solution. Figure 6 shows TEM images of the deposited Pt and PtNi bimetallic nanoparticles on the CNT surface. The TEM image analysis indicates that the mean particle size is between 2 and 16 nm but it increased from 3 to 15 nm by increasing the nickel content from 0 to 30 wt%. The particle morphology was mainly polygonal and hexagonal shapes. Also, the most important feature of the polyol process is the deposition of PtNi nanoparticles on the surface of CNTs without any intermediate molecule or nucleus as in the case of the sensitised method.[34–42]

In the second fabrication method of the Pt/CNTs and the related PtNi/CNT nanocomposites, G4 PAMAM dendrimer is anchored on the CNTs as a platform to load the Pt or PtNi nanoparticles, and sodium borohydride reacts as a reducing agent for the Pt and Ni ions. It is known that well-defined dendrimers with unique structures and compositions could be used to control the size, shape and solubility of Pt and PtNi nanoparticles on the surface of CNTs.[33] In the present study, after G4 PAMAM dendrimers attached to CNTs, Pt and PtNi nanoparticles with controlled size were fabricated. TEM images of the Pt/dendrimer/CNTs and the related PtNi/dendrimer/CNT nanoparticles are shown in Figure 7. It was found that the sizes of Pt/Ni bimetallic nanoparticles as well as Pt nanoparticles on dendrimer/CNTs ranged between 2 and 5 nm, and the mean particle size slightly increased from 3 to 4 nm by increasing the nickel content from 0 to 30 wt%.

In comparison with the first method, the deposited PtNi particles on the CNTs in the second method have smaller particle size. It may be related to the two types of roles of the dendrimer on the fabrication of metal nanoparticles which are known [42]: one is the nucleation of metal nanoparticles in dendrimers and the other is the protection of metal nanoparticles by dendrimers.[43,44] These prospects indicate that PAMAM dendrimers attached on CNTs play a role for controlling size of metal nanoparticles, agreeing with roles of free dendrimers as a size controller as well as a protector in the medium.[45]

The phase identification of the CNTs as well as the Pt/Ni nanoparticles was performed by XRD. XRD spectra for MWCNTs (Figure 8(a)) clearly reveal an intense peak at $2\theta \sim 25^\circ$ characteristic of CNTs containing the signature for reflection from (002) plane in addition to small intense peaks for (101), (220) and (110) planes for carbon.[46] Figure 8(b) shows two XRD patterns of two samples of PdNi/CNTs, synthesised by the polyol method and by dendrimer-intermediated method. The results proved their structural characterisation of the Pt and Ni face-centred cubic (FCC) pure phases. Three groups of diffraction peaks were appeared. The first group consists of five diffraction peaks of Pt included (111), (200), (220), (311) and (222). The second group consists of four diffraction peaks appeared due to the presence of Ni included (111), (200), (220) and (311) plans of Ni metal. The third group consists of the diffraction peaks of the presence of CNTs. It

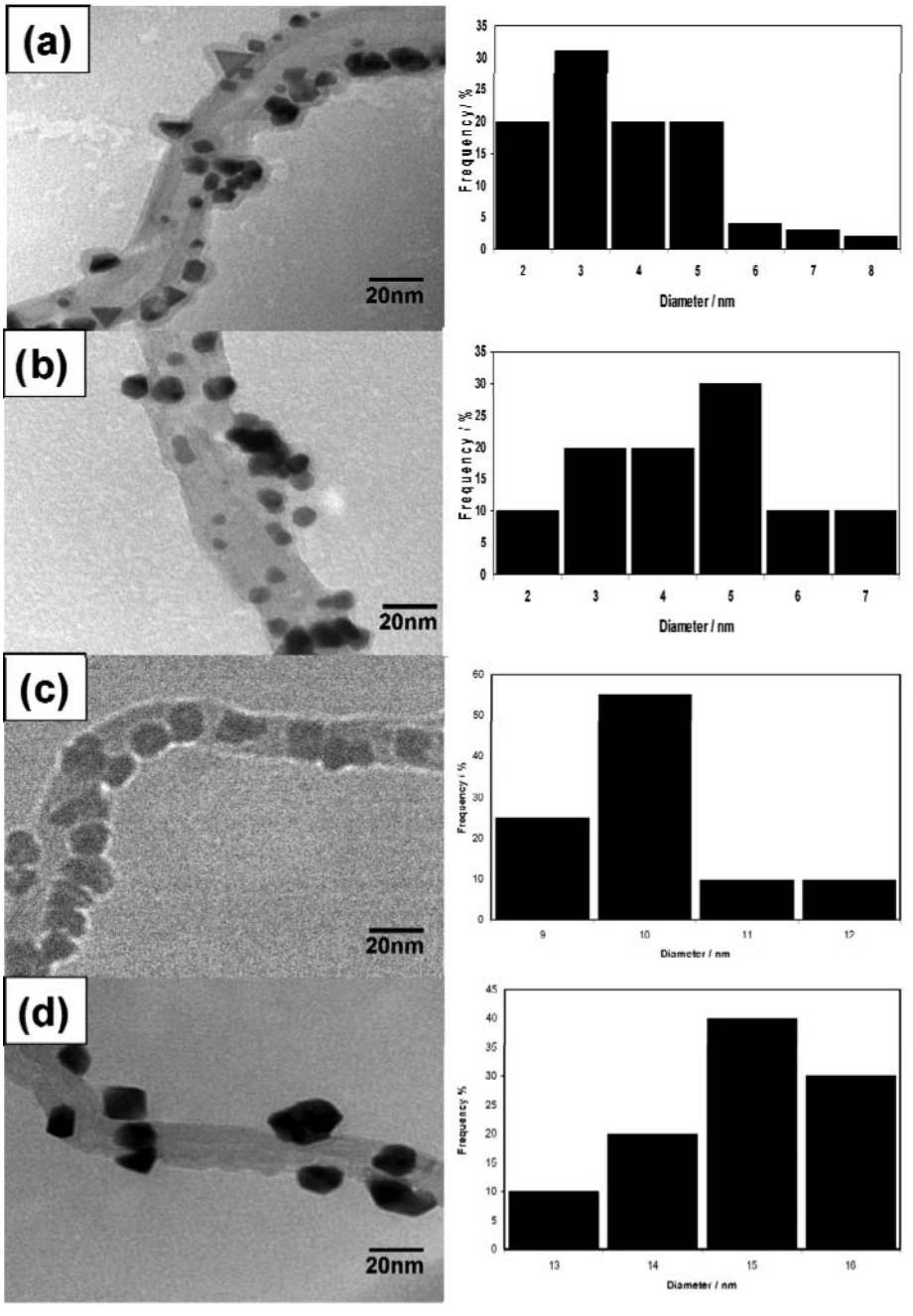

Figure 6. TEM micrographs and the related image analysis (size distribution) for nanoparticles prepared by polyol method: (a) Pt/CNTs, (b) 90PtNi/CNTs, (c) 80PtNi/CNTs and (d) 70PtNi/CNTs.

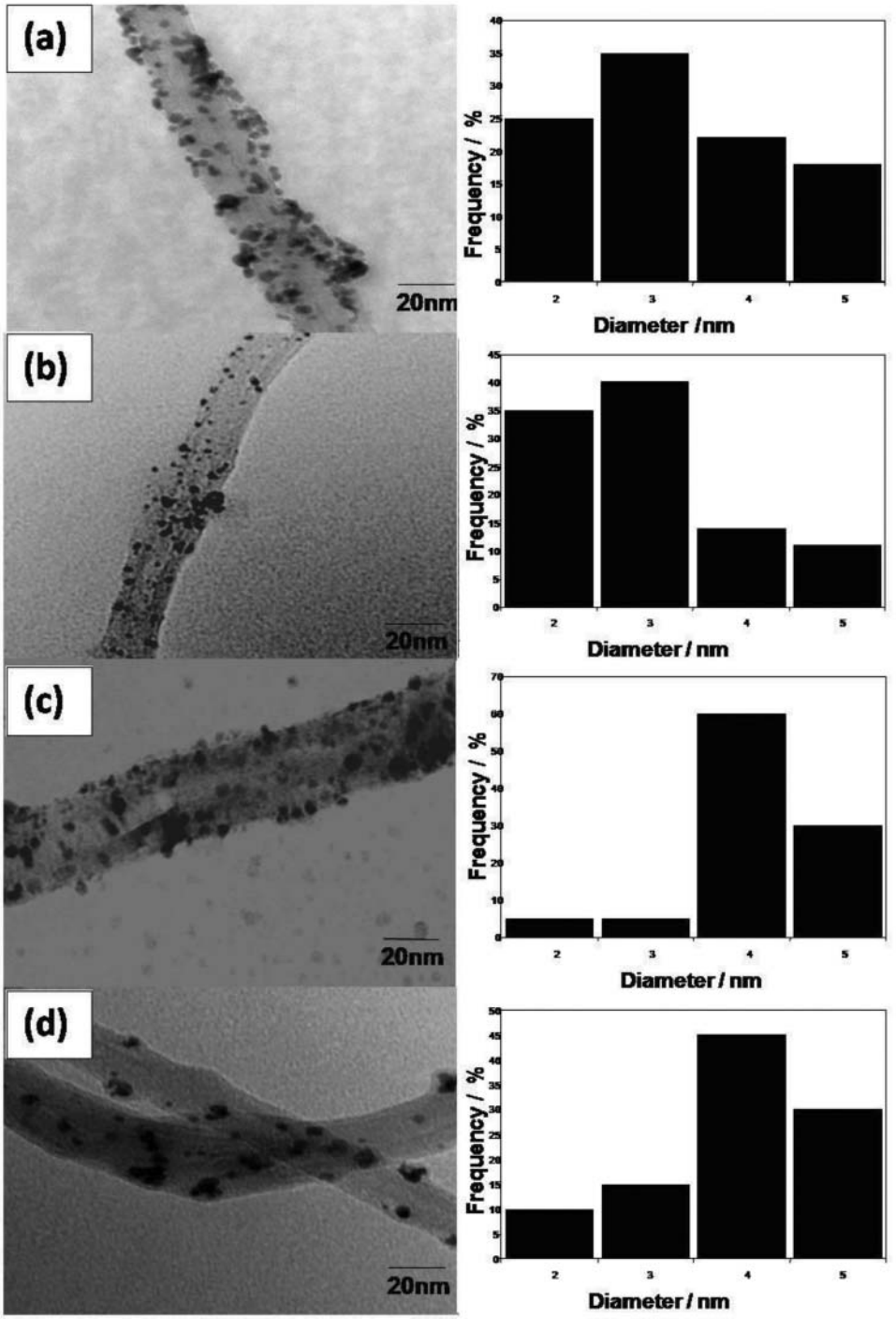

Figure 7. TEM micrographs and the related image analysis (size distribution) for nanoparticles prepared by dendrimer-intermediated method: (a) Pt/CNTs, (b) 90PtNi/CNTs, (c) 80PtNi/CNTs and (d) 70PtNi/CNTs.

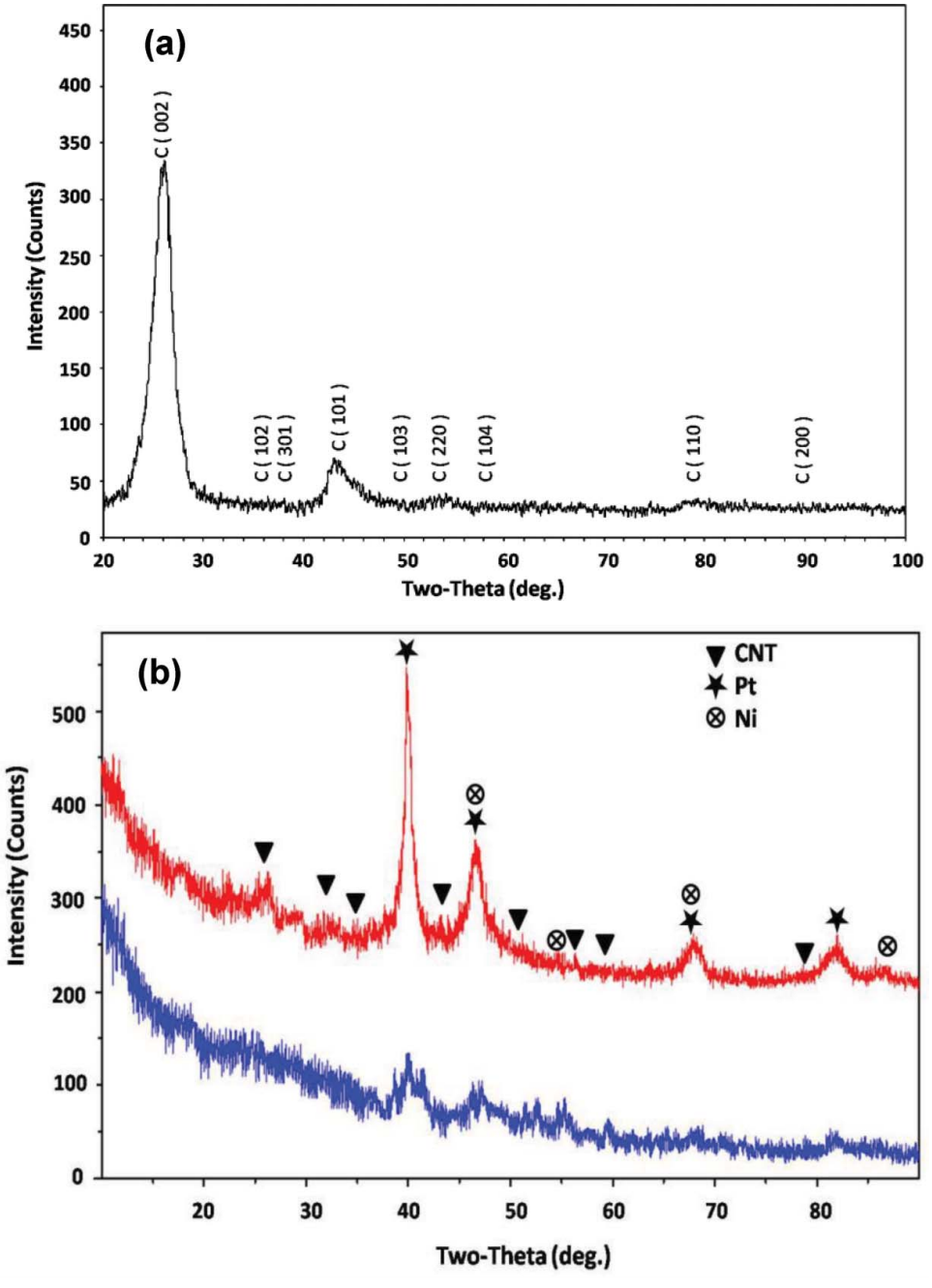

Figure 8. XRD patterns of the investigated nanoparticles: (a) MWCNTs and (b) the PtNi/CNT bimetallic nanoparticles prepared by polyol method (blue line) and the PtNi/CNT bimetallic nanoparticles prepared by dendrimer-intermediated method (red line).

was observed that the XRD patterns of PdNi/CNTs, synthesised by the polyol method and by dendrimer-intermediated method were similar in their appearance and shape, but the intensities of their diffraction peaks were different. The high intensity diffraction peaks appeared in the pattern of the PdNi/CNTs, synthesised by the dendrimer-intermediated method indicated that the Pt and Ni nanoparticles of a narrow shape distribution on the CNT substrate than the nanoparticles synthesised by the polyol method.[47]

UV–visible absorption spectrometry also elucidates the size change of Pt and PtNi nanoparticles depending on the fabrication method, as shown in Figure 9(a). Because of

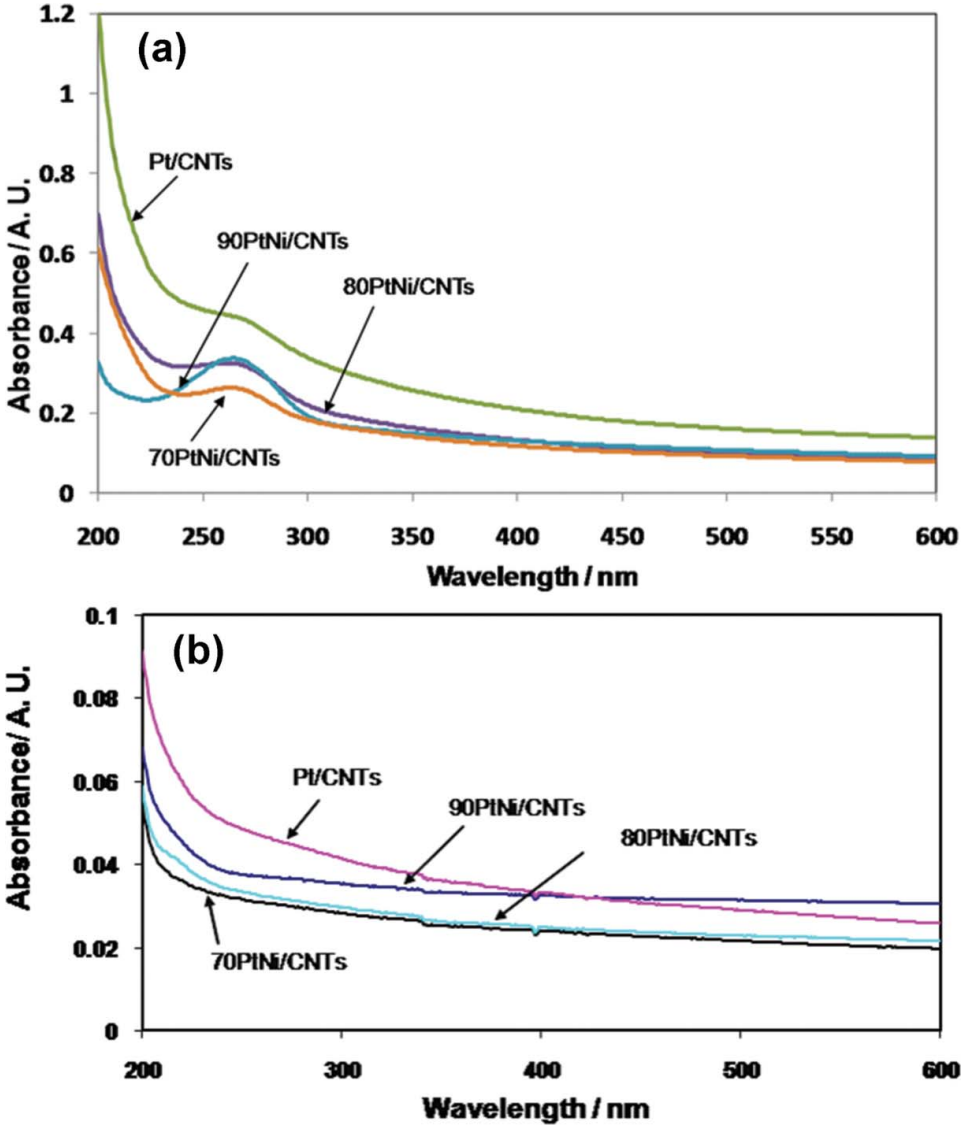

Figure 9. UV–visible absorption spectra of Pt/CNT and PtNi/CNT nanoparticles synthesised by (a) polyol method and (b) dendrimer-intermediated method.

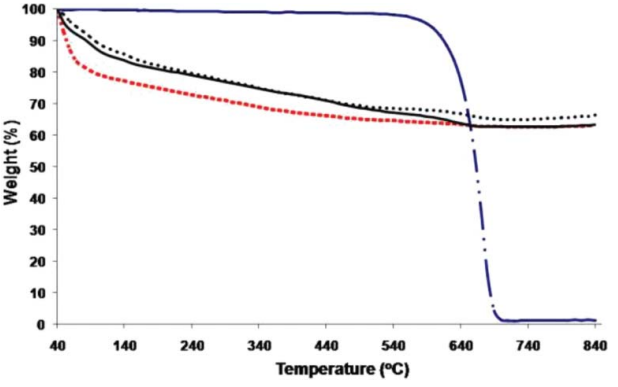

Figure 10. TGA of acid-treated CNTs (dotted line), Pt/CNTs (pink line), 90PtNi/CNTs, 80PtNi/CNTs (black line) and 70PtNi/CNTs (red line) nanoparticles synthesized by polyol method.

the presence of CNT, the background absorbance of all spectra monotonically increased toward low-wavelength side. The Pt/CNT and PtNi/CNT hybrids synthesised by a polyol method displayed a distinguishable, characteristic absorption band around 253 nm, which could be ascribed to the surface plasmon absorption band of Pt and Pt/Ni nanoparticles owing to the relatively large particle sizes (up to 16 nm) (Figure 9(a)). On the other hand, for Pt/CNT and PtNi/CNT nanoparticles synthesised under the coexistence of dendrimer, no characteristic absorption band appeared in the UV–visible absorption spectrum (see Figure 9(b)). Since the size of these particles is small (2–5 nm), the non-appearance of plasmon bands could be due to quantum dot size effect. These studies suggest that the particle size plays an important role on the spectroscopic characteristics of nanoparticles on CNTs.

The weight content of Pt and PtNi bimetallic nanoparticles could be determined by TGA. As shown in Figure 10, the acid-treated CNTs were decomposed at the temperature range of 600–700 °C in argon atmosphere (dashed line). On the other hand, Pt/CNT and PtNi/CNT nanoparticles were gradually decomposed up to 700 °C. On TGA curves (solid lines), the weight was about 64–67 wt% at 600 °C due to the decomposition of CNT. Then, from the weight loss in the TGA result, the weight content of the metallic nanoparticles (Pt or PtNi) was evaluated to be about 64–67 wt%. This value is consistent with the calculated ratio (70:30) (see Section 2).

4. Conclusion

Platinum and platinum/nickel supported, multi-walled CNT bimetallic nanoparticles have been fabricated by surface modification of the CNTs by acid treatment followed by two different deposition methods of the Pt and PtNi nanoparticles on CNT surfaces. The first one is the polyol method and in the second method dendrimer is used as a platform to load the nanoparticles. The loading was characterised by using a semi-quantitative analysis, that is, TGA. The synthesised PtNi/CNT bimetallic nanoparticles as well as Pt/CNT nanoparticles by both synthesis methods take the morphology of decorated-type CNTs by PtNi and Pt nanoparticles, respectively. The mean particle size of the deposited PtNi

nanoparticles on the CNTs increases by increasing the nickel content in the PtNi bimetallic nanoparticles. In addition, the PtNi nanoparticles deposited by the polyol method have larger mean particle size than the nanoparticles mediated by dendrimers. The PtNi/CNT nanoparticles synthesised by the dendrimer-intermediated method have a narrower particle size than the one synthesised by the polyol method. These Pt/CNT as well as the PtNi/CNT bimetallic nanoparticles should be available as electrocatalysts for direct methanol fuel cells.

Acknowledgements

The authors acknowledge the technicians at the Central Metallurgical R&D Institute in Cairo, Egypt for their help during the XRD analysis of the produced nanoparticles.

References

[1] Hamnett A. Mechanism and electrocatalysis in the direct methanol fuel cell. Catal Today. 1997;38:445–457.
[2] Sun X, Li R, Villers D, Dodelet JP, Désilets S. Composite electrodes made of Pt nanoparticles deposited on carbon nanotubes grown on fuel cell backings. Chem Phys Lett. 2003;379(1–2):99–104.
[3] Mu Y, Liang H, Hu J, Jiang L, Wan L. Controllable pt nanoparticle deposition on carbon nanotubes as an anode catalyst for direct methanol fuel cells. J Phys Chem B. 2005; 109(47):22212–22216.
[4] Ambrosio E, Francia C, Manzoli M, Nerino P. Platinum catalyst supported on mesoporous carbon for PEMFC. Int J Hydrogen Energy. 2008;33(3):3142–3145.
[5] Saha MS, Gulla AF, Allen RJ, Mukerjee S. High performance polymer electrolyte fuel cells with ultra-low Pt loading electrodes prepared by dual ion-beam assisted deposition. Electrochim Acta. 2006;51:4680–4692.
[6] Gamburzev S, Appleby A. Recent progress in performance improvement of the proton exchange membrane fuel cell (PEMFC). J Power Sources. 2002;107:5–12.
[7] Choi JH, Park KW, Park IS, Nam WH, Sung YE. Methanol electro-oxidation and direct methanol fuel cell using Pt/Rh and Pt/Ru/Rh alloy catalysts. Electrochim Acta. 2004; 50(2–3):787–790.
[8] Hyun MS, Kim SK, Lee B, Peck D, Shul Y, Jung D. Effect of NaBH4 concentration on the characteristics of PtRu/C catalyst for the anode of DMFC prepared by the impregnation method. Catal Today. 2008;132(1–4):138–145.
[9] Park KW, Choi JH, Kwon BK, Lee SA, Sung YE. Chemical and electronic effects of Ni in Pt/Ni and Pt/Ru/Ni alloy nanoparticles in methanol electrooxidation. J Phys Chem B. 2002;106:1869–1877.
[10] Park KW, Choi JH, Lee SA, Park C, Chang H, Sung YE. PtRuRhNi nanoparticle electrocatalyst for methanol electrooxidation in direct methanol fuel cell. J Catal. 2004;224(2):236–242.
[11] Samant PV, Rangel CM, Romero MH, Fernandes JB, Figueired JL. Carbon supports for methanol oxidation catalyst. J Power Sources. 2005;151:79–84.
[12] Samjeske G, Wang H, Loffler T, Baltruschat H. CO and methanol oxidation at Pt-electrodes modified by Mo. Electrochim Acta. 2002;47:3681–3692.
[13] Wu H, Wexler D, Wang G. PtxNi alloy nanoparticles as cathode catalyst for PEM fuel cells with enhanced catalytic activity. J Alloys Compdounds. 2009;488(1):195–198.
[14] Deivaraj TC, Chem W, Lee JY. Preparation of PtNi nanoparticles for the electrocatalytic oxidation of methanol. J Mater Chem. 2003;13:2555–2560.

[15] Lima A, Coutanceau C, Leger JM, Lamy C. Investigation of ternary catalysts for methanol electrooxidation. J Appl Electrochem. 2001;31:379–386.
[16] Liu F, Lee JY, Zhou W. Template preparation of multisegment PtNi nanorods as methanol electro-oxidation catalysts with adjustable bimetallic pair sites. J Phys Chem A. 2004;108:17959–17963.
[17] Antolini E, Salgado JRC, Giz MJ, Gonzalez ER. Effects of geometric and electronic factors on ORR activity of carbon supported Pt–Co electrocatalysts in PEM fuel cells. Int J Hydrogen Energy. 2005;30(11):1213–1220.
[18] Koh S, Yu C, Mani P, Srivastava R, Strasser P. Activity of ordered and disordered Pt-Co alloy phases for the electroreduction of oxygen in catalysts with multiple coexisting phases. J Power Sources. 2007;172(1):50–56.
[19] Travitsky N, Ripenbein T, Golodnitsky D, Rosenberg Y, Burshtein L, Peled E. Pt-, PtNi- and PtCo-supported catalysts for oxygen reduction in PEM fuel cells. J Power Sources. 2006;161:782–789.
[20] Antolini E, Salgado JRC, Gonzalez ER. The stability of Pt–M (M = first row transition metal) alloy catalysts and its effect on the activity in low temperature fuel cells: a literature review and tests on a Pt–Co catalyst. J Power Sources. 2006;160:957–968.
[21] Zignani SC, Antolini E, Gonzalez ER. Evaluation of the stability and durability of Pt and Pt–Co/C catalysts for polymer electrolyte membrane fuel cells. J Power Sources. 2008;182:83–90.
[22] Hsieh CT, Lin JY. Fabrication of bimetallic Pt–M (M = Fe, Co, and Ni) nanoparticle/carbon nanotube electrocatalysts for direct methanol fuel cells. J Power Sources. 2009;188(2):347–352.
[23] Nagle LC, Rohan JF. Aligned carbon nanotube composite deposition in platinum for fuel cell catalysts. J Power Sources. 2008;185:411–418.
[24] Hsieh CT, Hung WM, Chen WY. Electrochemical activity and stability of Pt catalysts on carbon nanotube/carbon paper composite electrodes. Int J Hydrogen Energy. 2010;35(16):8425–8432.
[25] Che G, Lakshmi BB, Martin CR, Fisher ER. Metal nanocluster-filled carbon nanotubules: catalytic properties and possible applications in electrochemical energy storage and production. Langmuir. 1999;15:750–758.
[26] Sun Y, Li C, Shi G. Nanoporous nitrogen doped carbon modified graphene as electrocatalyst for oxygen reduction reaction. J Mater Chem. 2012;22:12810–12816.
[27] Zou Y, Xiang C, Yang L, Sun LX, Xu F, Cao Z. A mediatorless microbial fuel cell using polypyrrole coated carbon nanotubes composite as anode material. Int J Hydrogen Energy. 2008;33:4856–4862.
[28] Sheng B, Hu L, Yu T, Cao X, Gu H. Highly-dispersed ultrafine Pt nanoparticles on graphene as effective hydrogenation catalysts. RSC Adv. 2012;2:5520–5523.
[29] Wang MY, Chen JH, Fan Z, Tang H, Deng GH, He DL, Kuang YF. Ethanol electro-oxidation with Pt and Pt–Ru catalysts supported on carbon nanotubes. Carbon. 2004;42:3257–3260.
[30] Han DM, Guo ZP, Zhao ZW, Meng YZ, Shu D, Liu HK. Polyoxometallate-stabilized Pt-Ru catalysts on multiwalled carbon nanotubes: influence of preparation conditions on the performance of direct methanol fuel cells. J Power Sources. 2008;184:361–369.
[31] Yamada H, Hirai T, Moriguchi I, Kudo T. A highly active Pt catalyst fabricated on 3D porous carbon. J Power Sources. 2007;164:538–543.
[32] Lu X, Imae T. Size-controlled in situ synthesis of metal nanoparticles on dendrimer-modified carbon nanotubes. J Phys Chem C. 2007;111:2416–2420.
[33] Guo Z, Chen Y, Li L, Wang X, Haller GL, Yang Y. Carbon nanotube-supported Pt-based bimetallic catalysts prepared by a microwave-assisted polyol reduction method and their catalytic applications in the selective hydrogenation. J Catal. 2010;276:314–326.
[34] Jafry HR, Whitsitt E, Barron AR. Silica coating of vapor grown carbon fibers. J Mater Sci. 2007;42(17):7381–7388.

[35] Daoush WM, Lim BK, Mo CB, Nam DH, Hong SH. Electrical and mechanical properties of carbon nanotube reinforced copper nanocomposites fabricated by electroless deposition process. Mater Sci Eng A. 2009;513–514:247–253.
[36] Scharf TW, Neira A, Hwang JY, Tiley J, Banerjee R. Self lubricating carbon nanotube reinforced nickel matrix composites. J Appl Phys. 2009;106(1):013508–013513.
[37] Okpalugo T, Papakonstantinou P, Murphy H, McLaughlin J, Brown N. High resolution XPS characterization of chemical functionalised MWCNTs and SWCNTs. Carbon. 2005;43:153–161.
[38] Liu Y, Tang J, Chen X, Chen W, Pang G, Xin JH. A wet-chemical route for the decoration of CNTs with silver nanoparticles. Carbon. 2006;44:381–383.
[39] Grolleaua C, Coutanceaua C, Pierreb F, Leger JM. Optimization of a surfactant free polyol method for the synthesis of platinum–cobalt electrocatalysts using Taguchi design of experiments. J Power Sources. 2010;195:1569–1576.
[40] Tsuji M, Matsumoto K, Jiang P, Matsuo R, Tang X-L, Kamarudin KS. Roles of Pt seeds and chloride anions in the preparation of silver nanorods and nanowires by microwave-polyol method. Colloids Surfaces A: Physicochem Eng Aspects. 2008;316:266–277.
[41] Dai K, Shi L, Fang J, Zhang Y. Synthesis of silver nanoparticles on functional multi-walled carbon nanotubes. Mater Sci Eng A. 2007;465:283–286.
[42] Tsuji M, Jiang P, Hikino S, Lima S, Yano R, Jang S-M, Yoon S-H, Ishigami N, Tang X, Kamarudin KS. Toward to branched platinum nanoparticles by polyol reduction: a role of poly (vinylpyrrolidone) molecules. Colloids Surfaces A: Physicochem Eng Aspects. 2008;317:23–31.
[43] Lu X, Imae T. Dendrimer-mediated synthesis of water-dispersible carbon-nanotube-supported oxide nanoparticles. J Phys Chem C. 2007;111:8459–8462.
[44] Siriviriyanun A, Imae T. Advantages of immobilization of Pt nanoparticles protected by dendrimers on multiwalled carbon nanotubes. Phys Chem Chem Phys. 2012;14:10622–10630.
[45] Daoush WM, Imae T. Syntheses and characterizations of multiwalled carbon nanotubes-supported palladium nanocomposites. J Mater Res. 2012;27(13):1680–2687.
[46] Hussain S, Pal AK. Incorporation of nanocrystalline silver on carbon nanotubes by electrodeposition technique. Mater Lett. 2008;62:1874–1877.
[47] Zhao J, Jarvis K, Ferreira P, Manthiram A. Performance and stability of Pd–Pt–Ni nanoalloy electrocatalysts in proton exchange membrane fuel cells. J Power Sources. 2011;196:4515–4523.